

Preparation of a Dual-Functionalized Acid–Base Macroporous Polymer via High Internal Phase Emulsion Templating as a Reusable Catalyst for One-Pot Deacetalization–Henry Reaction

Saeed Ghanooni, Babak Karimi, and Nasser Nikfarjam*

Cite This: *ACS Omega* 2022, 7, 30989–31002

Read Online

ACCESS |



Metrics & More

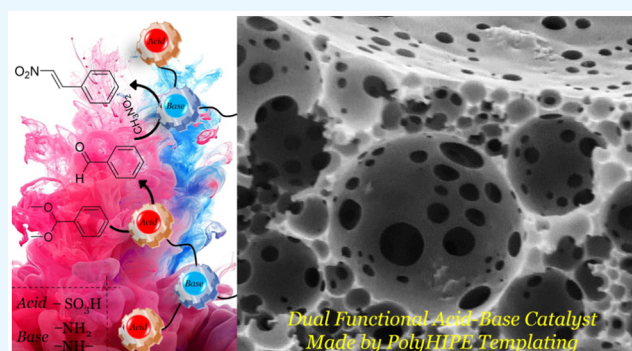


Article Recommendations



Supporting Information

ABSTRACT: A macroporous dual-functional acid–base covalent organic polymer catalyst poly(St-VBC)-NH₂-SO₃H was prepared using high internal phase emulsion polymerization using vinylbenzyl chloride (VBC), styrene (St), and divinylbenzene (DVB) as substrates toluene as a porogenic solvent, and subsequent modification with ethylenediamine and 1,3-propane sultone. The role of various amounts of toluene as the porogenic solvent as well as the amount of 1,3-propane sultone (different ratio of acid/base sites) on the structure of the prepared materials have been carefully investigated. The prepared materials were characterized by Fourier transform infrared (FT-IR), CHNS elemental analysis, energy-dispersive X-ray (EDX), elemental mapping, field emission scanning electron microscopy (FE-SEM), and thermogravimetric analysis (TGA). The catalytic activity of the poly(St-VBC)-NH₂-SO₃H series with different acid/base densities was assessed for one-pot cascade C–C bond-forming reactions involving deacetylation–Henry reactions. The poly(St-VBC)-NH₂-SO₃H(20) sample bearing 1.82 mmol/g of N (base site) and 1.16 mmol/g (acid site) showed the best catalytic activity. The catalyst demonstrated superior activity compared to the homogeneous catalysts, poly(St-DVB)-SO₃H+EDA, poly(St-VBC)-NH₂+chlorosulfonic acid, and poly(St-DVB)-SO₃H+poly(St-VBC)-NH₂ as the catalyst system. The optimized catalyst showed excellent catalytic performance with 100% substrate conversion and 100% yield of the final product in the one-pot production of β -nitrostyrene from benzaldehyde dimethyl acetal under cascade reactions comprising acid-catalyzed deacetalization and base-catalyzed Henry reactions. It was shown that these catalysts were reusable for up to four consecutive runs with a very slight loss of activity. The excellent performance of the catalyst was attributed to the excellent chemical and physical properties of the developed support since it provides an elegant route for preparing site-isolated acid–base dual heterogenized functional groups and preventing their deactivation via chemical neutralization.



1. INTRODUCTION

Recently, porous polymers have been received much attention because they elegantly combine the features of both porous materials and organic polymers including high surface area, flexible backbone, well-defined porosity, and easy synthesis and processing in different forms such as thin films, tabular, or individual spheres.^{1–3} There are various methods to develop porous polymer: phase-separation micromolding,⁴ high-internal phase emulsion polymerization,^{5,6} block copolymer,⁷ and particle or polymer leaching.⁸ Highly concentrated emulsions can be used as templates for the preparation of highly ordered porous polymeric structures. The high internal phase emulsions (HIPEs) technique is a versatile templating approach to produce porous polymers with interconnected channels and tunable pore size, which has been investigated extensively for the fabrication of porous materials with good moisture resistance, low cost, and a simple preparation process.^{9–11} Droplets in HIPEs are deformed because the

fraction of the dispersed phase is greater than 74 vol %, which corresponds roughly to the most compact hexagonal arrangement of uniform spherical droplets.^{12,13} Polymerization of precursors in the continuous phase of HIPE results in constructing a macroporous polymer (polyHIPE) with a 3D polymer skeleton induced by the emulsion template.^{14,15} In this technique, the morphology and pore structure of the monoliths are established by the state of the emulsion before the continuous phase is polymerized.¹⁶ Therefore, the stability of the emulsion has a critical influence on the final structure of the polymer and is determined by some factors like surfactant

Received: May 12, 2022

Accepted: August 12, 2022

Published: August 23, 2022



type and its concentration, temperature, processing conditions, and miscibility of the phases.

Several studies have been reported on how emulsion stability affects the cellular morphology.^{17–21} Notably, polyHIPE materials possess interconnected porous microstructures because the thin films between the droplets undergo shrinkage during the polymerization. This phenomenon creates interconnections, known as pore throats²² or voids,^{23,24} making polymer foams highly permeable. Although this phenomenon is the main reason for voids, some other methods such as post-thermal treatment and removing phase-separated surfactants assist the structure in creating new voids and enlarging the size of existing voids. Along this line, interesting studies on the effect of nonreactive diluents on the HIPE templating have highlighted the relationship between the solubility of the components and the morphology of the final polymeric structure.²⁵ For example, Cameron et al. added porogenic solvents to a divinylbenzene-based continuous phase during the HIPE templating process and have explored its effect on the resulting polyHIPE structure. They found that the pore architecture was influenced by the interaction of the solvent with the polymer network, the solvent polarity, and the degree of solvent adsorption at the O/W interface.²⁶

The cellular polymeric macro-structures have been widely used in separation and filtration media, tissue engineering scaffold, absorbent materials, microelectronics, controlled drug delivery, and chromatography.^{27,28} The wide-range applications of porous polymer structures stem from their broad functionality and range of properties (such as high surface area and low density), which can be easily achieved by introducing varied functional organic precursors and/or using multiple preparation methods.²⁹ In this context, many studies have recently utilized these macroporous polymers in the field of catalysis as catalyst support, owing to their interesting additional features, namely, the presence of interconnected microchannels in the macro-structure provided a suitable platform for efficient interaction of the reactants. In addition, these structures have the excellent capability to bear a range of functional groups, which can be introduced during the synthesis or via a postsurface modification approach. More importantly, the possibility of the large-scale synthesis of these materials in multiple shapes and morphologies is another eye-catching feature that would attract much attention for industrial catalytic reactions. Also, simple and efficient recovery of the prepared catalysts based on these macroporous polymers would make this process more green, economical, and environmentally benign.

Because of ever-increasing concerns over energy consumption, recently, one-pot cascade organic reactions have received considerable attention among organic chemists because they can simplify the operation and preparation processes, decrease the overall reaction time, and reduce the purification steps and the solvent consumption by running multiple reactions in a single operation setup.^{30–34} These features introduce the one-pot cascade reactions as a green, eco-friendly, and cost-effective process and thus present it as a valid candidate for developing “Green Chemistry” concepts. However, the great challenge in operating multiple catalytic reactions in the one-pot cascade system is providing appropriate reaction conditions that allow the suitable combination and efficient interaction of all substrates and catalytic substances without any interference, quenching, or occurrence of unwanted side reactions. In this regard, many homogeneous catalysts have been applied to

cascade reactions requiring dual acid–base functionalities.^{35–38} However, homogeneous catalytic systems have well-known product separation and reusability problems, increasing costs, and environmental impacts.³⁹ In addition, bifunctional acid–base catalytic activity is easily quenched in homogeneous reaction media owing to acid–base neutralization. To overcome these limitations and inspired by the site-isolation concepts, many researchers have recently pursued creating solid heterogeneous bifunctional acid–base catalysts by incorporating the acidic and basic functional groups in different locations of a single solid matrix.^{40–43} These engineered catalytic systems not only provide the best manner to prevent catalyst deactivation or quenching, particularly in the case of acid–base catalysts, but also present a well-defined platform for effective cooperation of several catalytic systems, as a single recoverable catalyst, in a series of one-pot cascade reactions. Several research groups have attempted to design such heterogeneous bifunctional cooperative acid–base catalysts by targeted and engineered immobilization of active molecules on multiple solid supports such as silica,^{44–49} heteropolyacids,³² metal–organic frameworks,^{50–52} metal oxides,⁵³ graphene oxide,⁵⁴ and covalent organic polymers⁵⁵ and their use in the cascade reactions.

Deacetalization–Henry cascade reaction is one of the most important and interesting cascade reactions that recently has attracted much attention among the organic chemists for operating in a one-pot process using recoverable acid–base cooperative catalysts.^{56,57} For example, bifunctional acid–base catalysts supported/immobilized on/in yolk–shell nanoreactors,^{49,58} MCM-41⁵⁹ and hexagonal mesoporous silica,⁶⁰ porous aromatic frameworks,⁵⁴ mesoporous hybrid nanocomposites,⁶¹ magnetic mesoporous silica,⁴⁷ double-shelled hollow mesoporous silica,⁶² poly(vinyl imidazole)/ZSM-5 composite,⁶³ and hollow nanospheres⁶⁴ have been employed successfully for catalyzing the deacetalization–Henry reaction. Along this line, recently bifunctional acid–base catalysts based on porous polymers have shown promising catalytic activity in the mentioned reaction because of their promising combined properties.^{65,66} In this regard, Yang et al. developed a novel concept based on a layered Pickering emulsion system which demonstrated efficient activity in catalyzing a series of one-pot cascade reactions, including the deacetalization–Henry reaction.⁶⁷ Also, very recently, well-designed polymeric core–shell microparticles containing an acidic site in the core and a basic site in the shell were developed by surfactant-free emulsion polymerization as an effective bifunctional catalyst for the deacetalization–Henry reaction.⁶⁸ Although the mentioned studies have shown promising achievements in developing bifunctional catalysts, there are still limitations from the material design viewpoint like using relatively complex preparation methods, the inability to synthesize the materials in large scale, and the lack of recoverability of the catalysts that should be resolved in future studies.

Taking care of these criteria and putting a step forward in designing new recoverable bifunctional catalyst, herein, we developed a series of macroporous dual-functional acid–base covalent polymers denoted as poly(VBC-St)-NH₂-SO₃H using high internal phase emulsions polymerization of vinyl benzyl chloride (VBC), styrene (St), and divinylbenzene (DVB) in the presence of toluene as a porogenic solvent followed by surface-functionalization by ethylenediamine and then propane sulfone. Furthermore, the physicochemical properties of the prepared bifunctional polymer macrostructures, and their

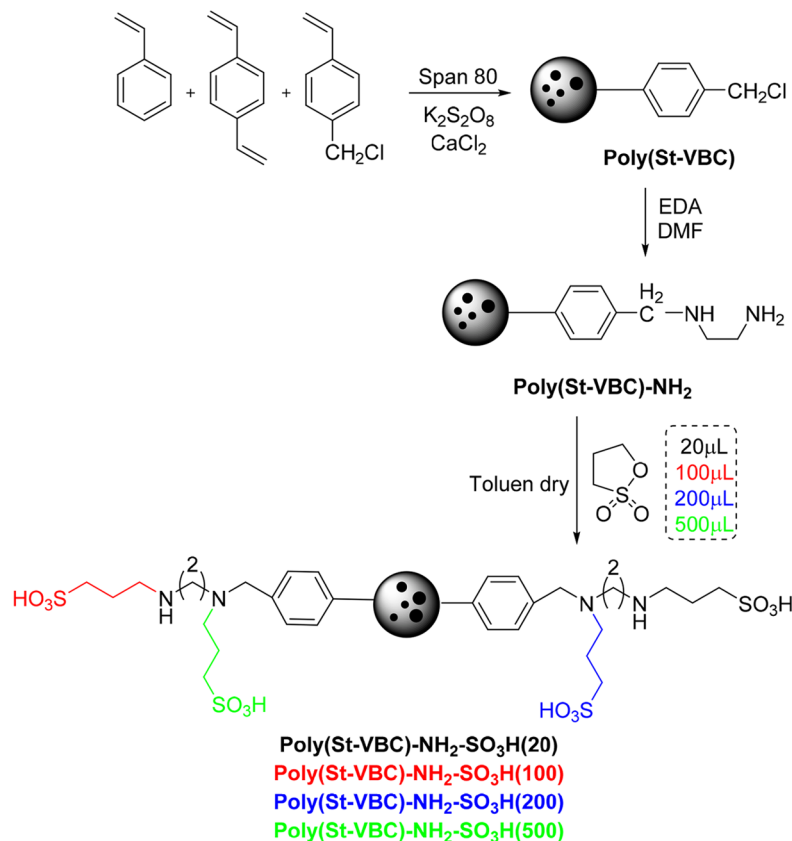
Scheme 1. Preparation of Poly(St-VBC)-NH₂-SO₃H(20–500)

Table 1. Formulated HIPE Emulsions to Prepare Poly(St-VBC) Samples Containing Different Amounts of Toluene as a Porogenic Solvent^a

Sample	VBC ^b (mmol)	DVB ^b (mmol)	St ^b (mmol)	Toluene ^b (mmol)	St/VBC	St+VBC/DVB	ϕ_{water} (V%)	ϕ_{oil} (V%)
Poly(St-VBC)- <i>T</i> = 0	0.63	0.42	1.3	0	2.06	4.6	80	20
Poly(St-VBC)- <i>T</i> = 50	0.63	0.42	1.3	0.4	2.06	4.6	80	20
Poly(St-VBC)- <i>T</i> = 100	0.63	0.42	1.3	0.9	2.06	4.6	80	20
Poly(St-VBC)- <i>T</i> = 150	0.63	0.42	1.3	1.3	2.06	4.6	80	20

^aThe following materials were used for all emulsions; K₂S₂O₈ (0.0015 wt % related to the water phase) as initiator, span 80 (20 wt % related to the oil phase) as a surfactant, and CaCl₂·2H₂O (0.016 wt % related to the water phase) as a preventer of Ostwald ripening phenomenon. ^bRelated to the oil phase.

catalytic activities in the one-pot deacetalization–Henry reaction have been investigated precisely.

2. EXPERIMENTAL SECTION

2.1. Materials. 4-Vinylbenzyl chloride (VBC), divinylbenzene (DVB, 80%), and chlorosulfonic acid were purchased from Sigma-Aldrich. Also, styrene, Span-80 (sorbitan monooleate, HLB = 4.3), potassium persulfate (K₂S₂O₈), calcium chloride dihydrate (CaCl₂·2H₂O), methanol, dimethylformamide (DMF), ethylenediamine (EDA), benzaldehyde dimethyl acetal, nitromethane, malononitrile, ethanol, and toluene were purchased from Merck and were used as received without further purification. Distilled water was used for all experiments.

2.2. Synthesis of Catalysts. **2.2.1. Synthesis of Macroporous Polymer Materials (Poly(St-VBC)).** The macroporous materials were synthesized through HIPE templating based on styrene, vinylbenzyl chloride, and divinylbenzene. The initial polyHIPE was obtained by copolymerization of 4-vinylbenzyl

chloride, styrene, and divinylbenzene in the presence of toluene as a porogenic solvent in the continuous phase of water-in-oil high internal phase emulsion stabilized by span 80 (Scheme 1). The detailed synthesis procedure is presented in Table 1. For example, for the poly(St-VBC)-*T*=100 sample, 4-vinyl benzyl chloride (0.63 mmol), styrene (1.30 mmol), divinylbenzene (0.42 mmol), toluene (0.9 mmol), and span 80 (20 wt %) were mixed in a PET mold (vial 5 mL) and stirred at 600 rpm for 30 min. The mixture was purged for 10 s with nitrogen, and then an aqueous solution containing K₂S₂O₈ and CaCl₂ (also purged with nitrogen) was added dropwise over 20 min under stirring of 600 rpm. The water-in-oil emulsion type was determined by the conductivity measurement (Metrohm 712, Switzerland) and drop test. Finally, the vial was sealed thoroughly with Teflon tape to prevent air from entering the emulsion and also evaporation of monomers and solvents. The emulsion in a PET mold was cured at 70 °C for 24 h followed by Soxhlet extraction with deionized water and then toluene (48 h with a circulating time of around 20 min for each extraction) and dried in an oven at 60 °C for 24 h. The

extraction with water and toluene was used, respectively, to remove CaCl_2 /residual of $\text{K}_2\text{S}_2\text{O}_8$ initiator and unreacted monomers. The size of at least 400 pores was manually measured by JMicrovision 1.2.7 software, and each data point was multiplied by a factor $k = 2/\sqrt{3}$ to have a better estimation of the real pore diameter.⁶⁸ Then the average diameter of pores (\bar{d}) was calculated from the equation $\bar{d} = \sum n_i d_i / \sum n_i$ where n_i is the number of pores with a diameter of d_i .

2.2.2. Determination of Chloride Content. The chloride content of all the manufactured polyHIPEs was determined through potentiometric titration. First, 0.02–0.03 g of materials was mixed with 5 mL of pyridine in a 10 mL round-bottomed flask and heated under reflux for 2 h at 90 °C. After cooling, the mixture was transferred to a 50 mL volumetric flask followed by the addition of 10 mL of DMF and 7 mL of nitric acid. Finally, the mixture was diluted with water to 50 mL, and the content of chloride was determined through potentiometric titration using 0.001 M AgNO_3 . For titration, 20 mL aliquots were used, and the chloride content was calculated from the required amount of AgNO_3 .

2.2.3. Synthesis of Poly(St-VBC)- NH_2 - SO_3H . Three class of catalysts were synthesized as follows: catalysts bearing only acid sites (Poly(St-DVB)- SO_3H , see the Supporting Information for details of the synthesis), catalysts bearing only base sites (Poly(St-VBC)- NH_2), and catalysts bearing both base and acid sites simultaneously (Poly(St-VBC)- NH_2 - SO_3H). For poly(St-VBC)- NH_2 samples, fresh poly(St-VBC)- $T=100$ (0.10 g) was added to 5 mL of DMF, and it was mildly stirred at room temperature for 1 h. Then ethylenediamine (EDA) (150 mmol) was added slowly, and the mixture was stirred at room temperature for another 1 h. Finally, the solid mixture was slowly stirred at 70 °C for 24 h (Scheme 1). In the end, the mixture was filtered and washed successively with DMF, ethanol, ethanol/ H_2O (ratio volume 1:1), ethanol/THF (ratio volume 1:1), and THF (3 mL \times 3) and finally dried in a vacuum oven at 60 °C for 24 h to yield poly(VBC-St)- NH_2 .⁶⁹

For poly(St-VBC)- NH_2 - SO_3H samples, 0.05 g of poly(St-VBC)- NH_2 was placed in 30 mL of dry toluene and slowly stirred at 60 °C for 2 h under argon atmosphere (Scheme 1). Next, 1,3-propane sultone (20, 100, 200, 500 μL) dissolved in 2 mL of toluene was added dropwise into the poly(St-VBC)- NH_2 suspension over 20 min, and the resulting mixture was stirred for 24 h at 60 °C. Then the mixture was filtered and washed with distilled toluene (3 mL \times 6) and ethanol (3 mL \times 6), and dried in the vacuum oven at 60 °C to yield, respectively, poly(St-VBC)- NH_2 - SO_3H (20), poly(St-VBC)- NH_2 - SO_3H (100), poly(St-VBC)- NH_2 - SO_3H (200) and poly(St-VBC)- NH_2 - SO_3H (500).

2.3. Catalytic Reactions. **2.3.1. One-Pot Deacetylation–Hercal Reaction.** In a typical reaction, benzaldehyde dimethyl acetal (1 mmol), poly(St-VBC)- NH_2 - SO_3H (X) (20 mg), nitromethane (5 mL), and H_2O (20 μL) were mixed in a reaction tube fitted with a condenser. The reaction mixture was kept at 90 °C under magnetic stirring for 24 h (the reaction was carried out under nitrogen gas flow), and aliquots of the reaction mixture were extracted using a filter syringe and analyzed on a gas chromatographer equipped with an CP-Sil 8 CB (25m \times 0.32 mm \times 1.2 μm) column to determine the conversion and yield of *trans*- β -nitrostyrene.

2.4. Characterization. **2.4.1. Fourier-Transform Infrared Spectroscopy (FT-IR).** The poly(St-VBC), poly(St-VBC)- NH_2 , and poly(St-VBC)- NH_2 - SO_3H were characterized using FT-IR

spectroscopy (Bruker vector 22 spectrophotometer, Germany) by preparing their KBr pellets from 400 to 4000 cm^{-1} . The samples were dried before characterization with a vacuum oven at 60 °C for 24 h.

2.4.2. Thermogravimetric Analysis (TGA). The thermal properties and composition of the prepared polyHIPEs were investigated using thermogravimetric analysis (NETZSCH STA 409 PC/PG) under an N_2 atmosphere with a flow rate of 20 mL/min and a heating rate of 10 °C/min from 30 to 800 °C. The samples were dried before characterization with a vacuum oven at 60 °C for 24 h.

2.4.3. Elemental Analysis. The chemical compositions of the obtained materials were determined by using a C–H–N–S elemental analyzer (Vrio EL III, Elementar Germany). The samples were dried before characterization with a vacuum oven at 60 °C for 24 h.

2.4.4. FE-SEM Analysis of PolyHIPE Macroporous Polymers. The prepared polyHIPEs were cut, coated with a gold layer, and then imaged by the field emission scanning electron microscopy (FE-SEM, Hitachi S4160 operating at 20 kV) to investigate the surface morphology and pore size.

2.4.5. Porosity. The porosity of polyHIPE macroporous was determined manually using the following equation; $\rho = 1 - (\rho_{\text{foam}}/\rho_{\text{bulk}}) \times 100$, where ρ_{foam} and ρ_{bulk} were, respectively, the density of foam (prepared polyHIPEs) and bulk state of the synthesized polymer based on St, VBC, and DVB monomers through bulk polymerization in the same molar ratio of monomers used for the synthesis of polyHIPE. Both samples (polyHIPE and bulk polymer) were cut in a defined cubic shape, and then their weight, volume, and densities were measured. The measurements were replicated, and average density values and errors were reported.

3. RESULTS AND DISCUSSION

3.1. Synthesis of Materials. The poly(St-VBC)- NH_2 - SO_3H materials were prepared via the following three-step procedure according to the presented routes in Scheme 1: (a) synthesis of poly(St-VBC) through HIPE templating method using styrene, 4-vinylbenzyl chloride, divinylbenzene as cross-linker, and toluene as a porogenic solvent; (b) modification of poly(St-VBC) with ethylenediamine in DMF to give poly(St-VBC)- NH_2 , and (c) functionalization of poly(St-VBC)- NH_2 with various amounts of 1,3-propane sultone (20, 100, 200, 500 μL) in dry toluene to prepare poly(St-VBC)- NH_2 - SO_3H catalysts with different acid contents. The chloride content of poly(St-VBC) was first precisely determined (15.35 mmol/g), and then the ethylenediamine content was used in around 100 \times molar excess based on the determined chloride content of materials to ensure the complete reaction of chloride functionality.

3.2. Catalyst Characterization. The surface area of the polyHIPE compounds increases remarkably by combination of three factors: (1) high cross-linker level, (2) an inert diluent (porogen) added to the continuous phase containing monomers, and (3) a high-level surfactant concentration.^{70,71} In this work, the cross-linking degree and surfactant content were kept constant as high as possible and the effect of toluene as a porogen agent was investigated. In this mechanism, after dissolving the porogenic solvent in the reaction medium and completing the polymerization process, the porosity in the final polymer increases after washing and removing the porogenic solvent. Basically, porosity arises from the phase separation from the porogen and the growing polymer chains during

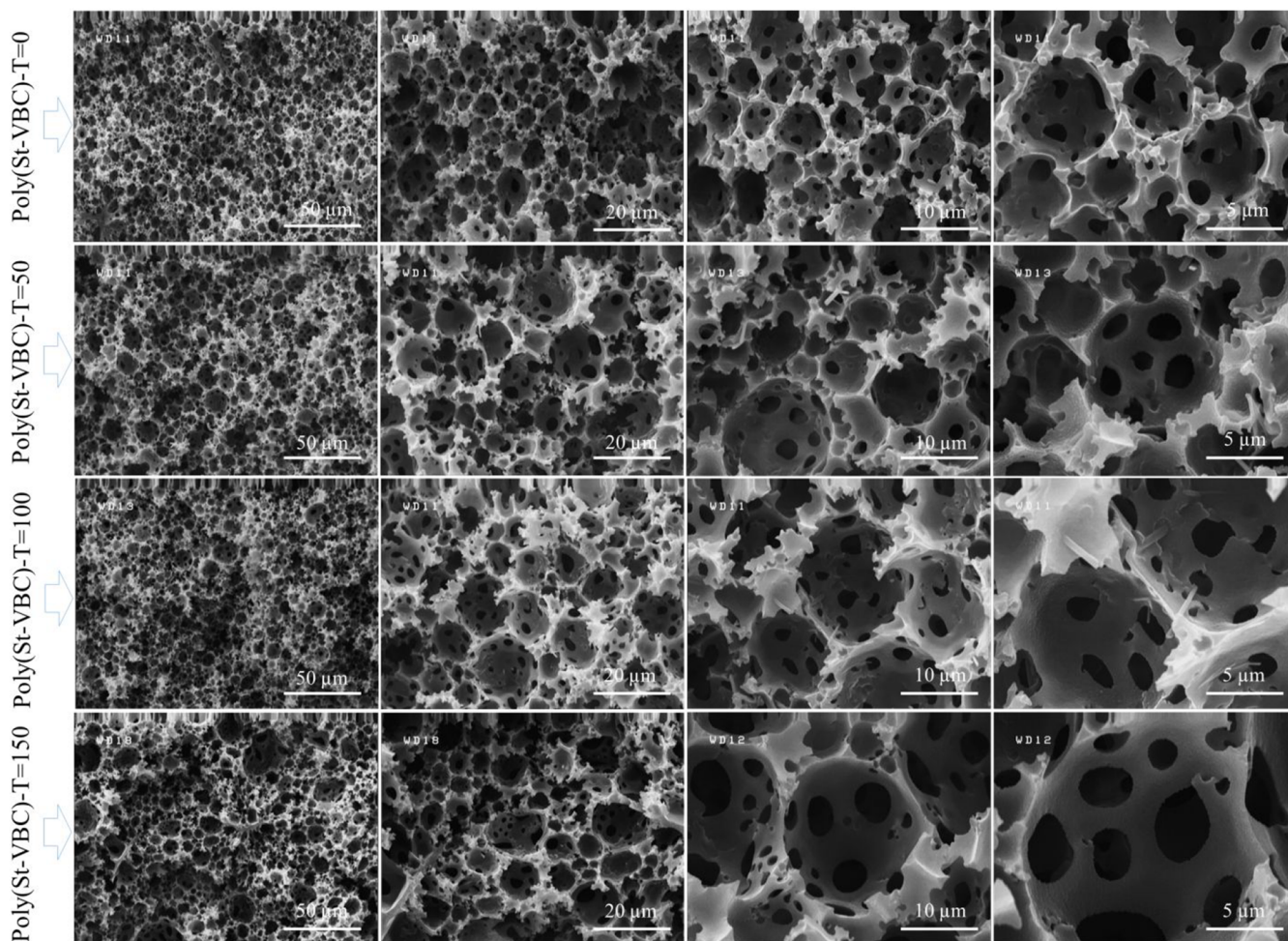


Figure 1. FE-SEM images on the cross-sectional area of poly(St-VBC)-*T* obtained by HIPE templating with different amounts of toluene as porogenic solvent (*T* refers to the amount of toluene added to the formulation, and it ranges from 0, 50, 100, to 150 μL).

polymerization.⁷¹ Porogens with a low solubility undergo early phase separation and tend to form larger pores and, therefore materials with lower surface areas. Conversely, porogens with higher phase solubility separate late in the polymerization to provide materials with smaller pore size distributions and greater surface area.⁷¹

Based on the literature and our experiments, the macroporous polymer prepared by toluene as a porogen solvent showed a better appearance, structural integrity, and no chalky materials. We performed further experiments to investigate the effect of toluene solvent on the morphology of pores and pore size and void size distributions.⁷¹

To investigate the exact role of toluene as the porogenic solvent, we prepared various samples with different amounts of toluene ($T = 0, 50, 100, 150 \mu\text{L}$). The manual measurements and calculations revealed that the porosity of the poly(St-VBC)- $T=0$, poly(St-VBC)- $T=50$, poly(St-VBC)- $T=100$, and poly(St-VBC)- $T=150$ was, respectively, 80 ± 1.4 , 84 ± 1.7 , 96 ± 1.2 , and $90 \pm 1.9\%$. Also, the morphology of the obtained materials was examined by using field emission scanning electron microscopy (FE-SEM). Our preliminary observations revealed that as the toluene content increases the total porosity of the poly(St-VBC)- T increases (Figure 1). The evaluation of FE-SEM images well showed that the pore and void size were increased by increasing the toluene amount and therefore decreasing monomer content (Figure 1). Also, the statistical

analysis on the structures exhibited that the numerical distribution of pore and void sizes has shifted to the higher values with decreasing monomer content and increasing toluene content (Figure 2A,C, Figures S1 and S2). The calculated average pore and void size increased gradually with decreasing monomer content or decreasing toluene content. With the increase in the toluene content, the average pore size increased from 5.5 to 7.5 μm (Figure 2B), and the average void size increased from 1.1 to 1.5 μm (Figure 2D). The reason lies in forming a thin polymer layer around the droplets in the high content of toluene or low content of monomers. Therefore, the high shrinkage rate of this polymeric thin layer around the droplets can lead to bigger voids. Also, the coalescence probability of droplets during the polymerization can be enhanced due to the diminished strength of the formed thin polymer layer leading to the larger pores. Another reason that can be considered is the low viscosity of the continuous phase, permitting the droplets to find each other and fuse easier (coalescence phenomenon) to form the larger droplets and consequently the larger pores and voids in the final macroporous structure, while in the samples with low toluene content the droplet mobility and penetration are limited due to the high viscosity of the continuous phase of the emulsion, leading to the smaller pores and voids in the final macroporous structure. Assuming Stokes' law $D_{\text{diff}} = k_{\text{B}}T/6\pi\eta r^3$ is applicable here (where k_{B} is the Boltzmann constant, T is the absolute

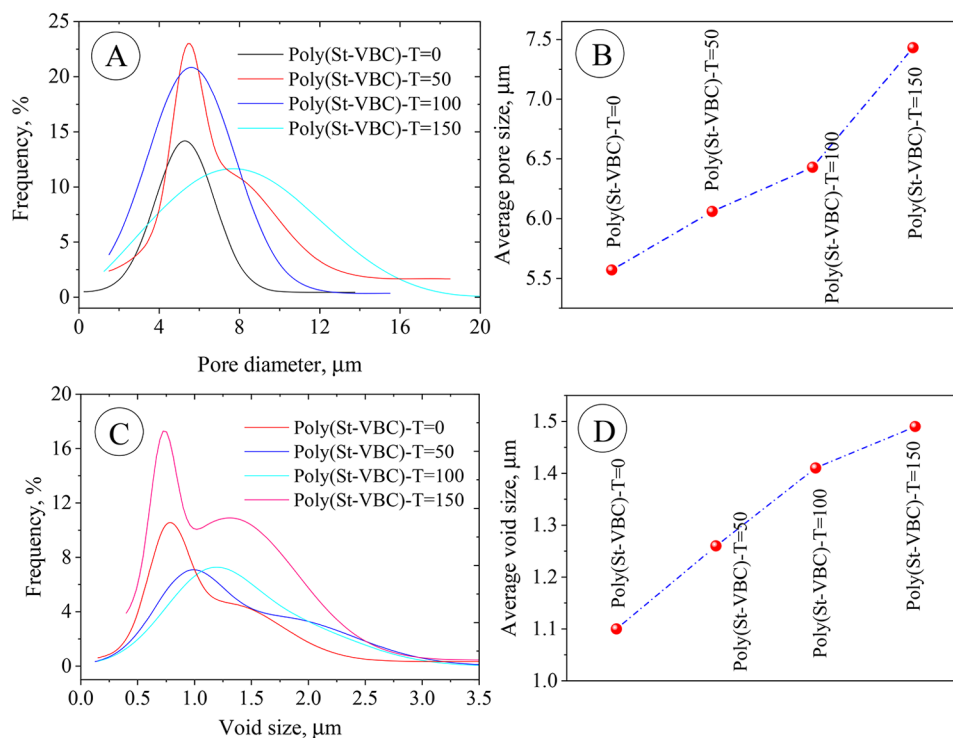


Figure 2. Number distribution of pore (A) and void (C) and also calculated average of pore size (B) and void size (D) of prepared macroporous poly(St-VBC)-*T* with different content toluene (*T* refers to the amount of toluene added to the formulation and ranges from 0, 50, 100, to 150 μL). The data were fitted by Gaussian equation using OriginPro v.9.2. software.

temperature, η is the continuous phase viscosity, and r is the radius of the droplets^{72–74}), the higher viscosity of the continuous phase of the emulsion leads to the lower diffusion coefficient (D_{diff}), and thus, the probability of droplet collision and coalescence is reduced.

The integrity of the obtained macroporous structures was diminished with increasing toluene content (decreasing monomers content) due to the increasing number and size of pores and voids. Thus, the higher content of toluene in the sample poly(St-VBC)-*T*=150 resulted in a chalky structure. This issue may reduce the applicability of macroporous polymer materials with too high porosity and weak mechanical strength.

Toluene, as porogen solvent, significantly affects the surface morphology of pores. FE-SEM images demonstrated that as the toluene content increases, pores' uniformity and internal surface morphology are changed from smooth to rough. In the case of poly(St-VBC)-*T*=0, the inner surface of pores is perfectly smooth and uniform, while it turns to the rough and protruded morphology for the samples containing toluene (Figure 3). As the toluene content increases, polymer and solvent-rich regions are formed due to the possible phase separation in the polymeric layer around the droplets during the polymerization, resulting in a rough surface on the inner surface of pores.⁷⁵ Consequently, the surface area of pores increases dramatically with an increase in the pore's roughness. This enhanced surface area is an interesting feature of these polymeric macroporous materials for their catalytic application purposes.

Our findings showed that the porogen solvents (here, toluene) positively affected the porosity. However, in the higher content of toluene, the samples lost their integrity. Based on these results, one could conclude that the sample

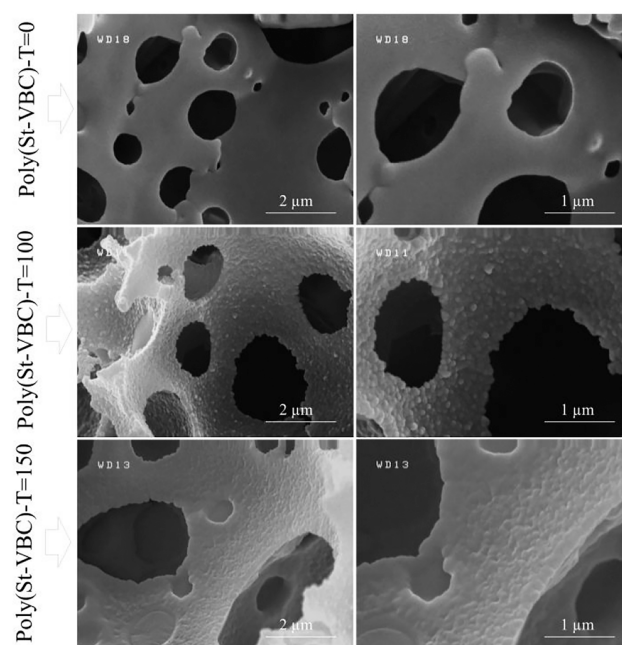


Figure 3. FE-SEM images of surface of inner wall of pores in poly(St-VBC)-*T*=0, poly(St-VBC)-*T*=100, and poly(St-VBC)-*T*=150.

poly(St-VBC)-*T*=100 could be a good candidate as a solid substrate for catalytic applications due to its high porosity and surface area. Therefore, the macroporous sample poly(St-VBC)-*T*=100 was first modified with ethylenediamine followed by modification with 1,3-propane sultone (Scheme 1) to obtain dual-functional catalysts containing active acid–base sites simultaneously. The following parameters are very

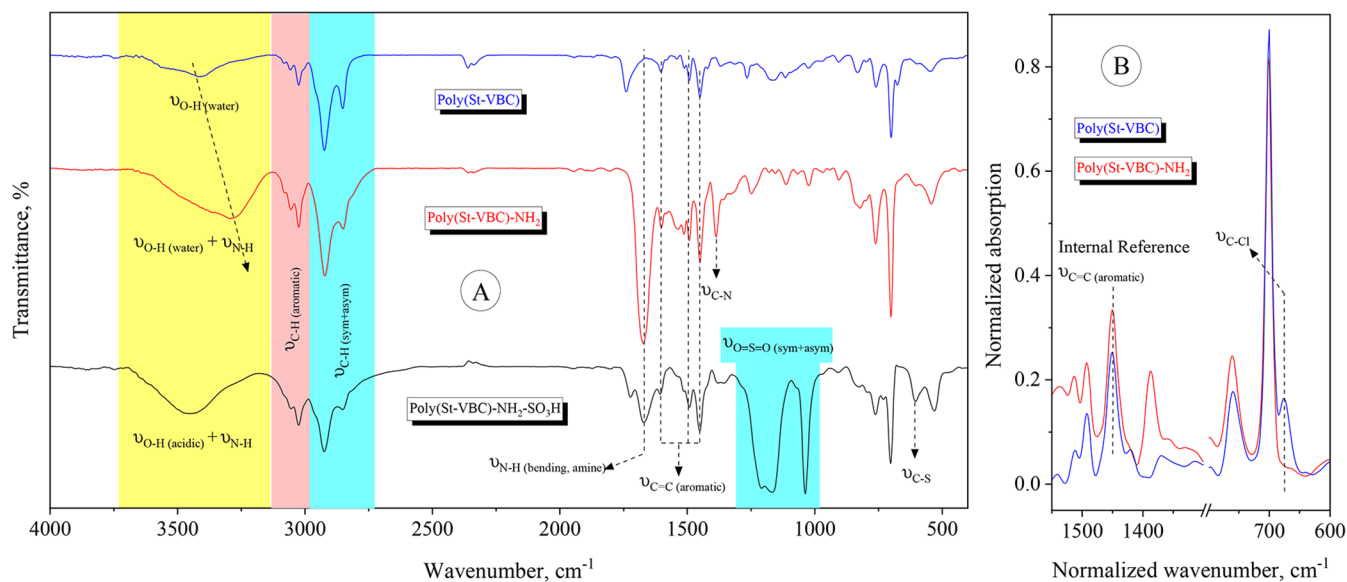


Figure 4. (A) FT-IR spectra of poly(St-VBC), poly(St-VBC)-NH₂, and poly(St-VBC)-NH₂-SO₃H(20) and (B) extended normalized absorption spectra in 800–500 cm⁻¹.

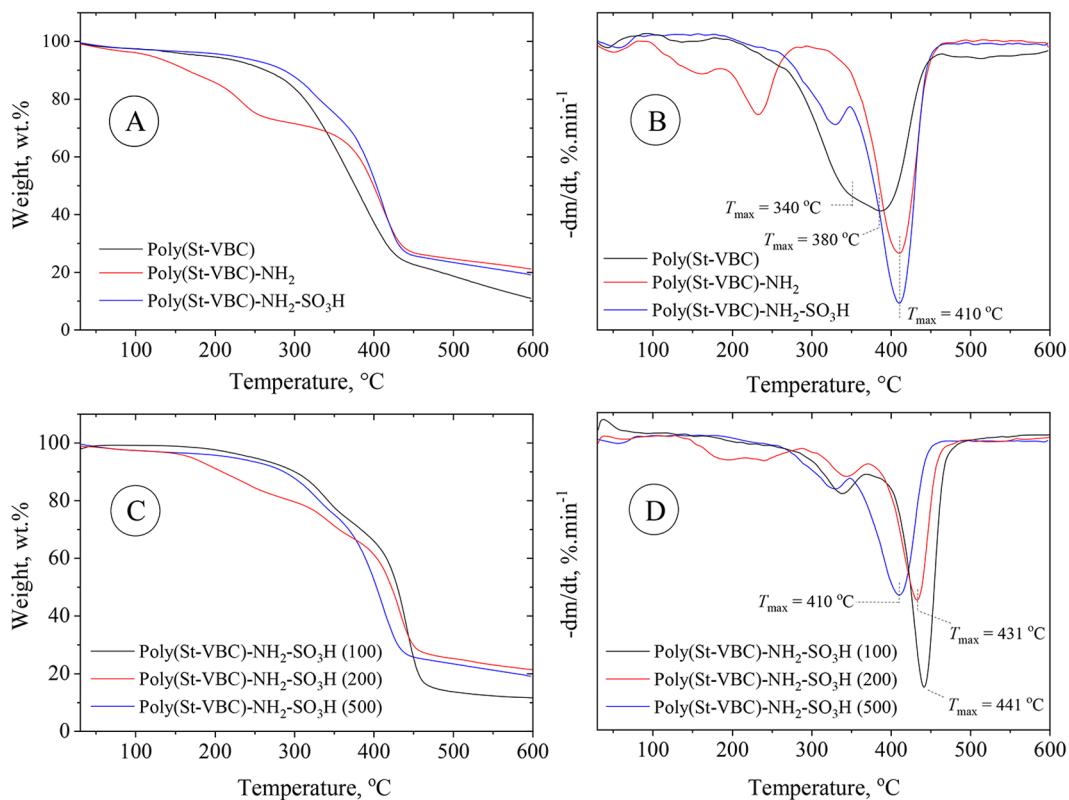


Figure 5. Thermogravimetric analysis (TGA) (A and C) and differential thermogravimetric analysis (DTG) (B and D) of the prepared macroporous polymer catalysis.

effective in the tandem reactions that should be considered: the surface area of catalyst, the density of active acid–base sites, the distance between active sites, and homogeneously dispersed active sites on the structure.⁴⁸

The FT-IR spectra showed that the functionalities of –NH₂ and –SO₃H were grafted on the porous structure, and therefore, it was found that the samples poly(St-VBC), poly(St-VBC)-NH₂, and poly(St-VBC)-NH₂-SO₃H were

successfully synthesized (Figure 4A). In more detail, the observed peak at about 1492, 1450, 1602 cm⁻¹ in all of the spectra characteristic of an aromatic ring confirmed the aromatic nature of the main skeleton of all substrates resulted from styrene, vinylbenzyl chloride, and divinylbenzene. Also, the peaks at 2850–2950 and 674 cm⁻¹ are related, respectively, to the stretching vibration of aliphatic C–H and C–Cl.⁷⁶ After functionalization of poly(St-VBC) with ethylenediamine, new

characteristic peaks are observed for stretching vibrations of C–N (1386 cm^{-1}) and bending vibration of N–H aliphatic amines, while the intensity of peak related to the C–Cl was dramatically decreased (Figure 4B). In addition, the broad peak at 3000–3600 cm^{-1} is shifted to the lower wavenumbers due to addition of aliphatic amines to the structures. It is believed that this broad peak results from overlapping of stretching vibration of N–H amines occurs at 3310–3350 cm^{-1} and stretching vibration of O–H occurs around 3400 cm^{-1} caused by the trapping of water molecules during the washing process.^{77,78} These results proved that the EDA is successfully grafted onto poly(St-VBC).^{79,80} The dual-functionalized poly(St-VBC)-NH₂-SO₃H showed O=S=O stretching vibrations (symmetric and asymmetric) at 1027–1214 cm^{-1} and stretching vibration of C–S at 626 cm^{-1} relating to the sulfonic acid group, indicating the presence of a –SO₃H group attached to the amine moiety of the substrate through propyl chain.^{81,82}

The stretching vibration of aromatic C=C occurred at 1450 cm^{-1} was considered as internal reference (Figure 4B) and substitution degree of chloride by ethylenediamine was calculated according to the following equation

$$\text{degree of substitution(\%)} = \left[1 - \frac{\left(\frac{I_{1450}}{I_{674}} \right)_{\text{Poly(St-VBC)}}}{\left(\frac{I_{1450}}{I_{674}} \right)_{\text{Poly(St-VBC)-NH}_2}} \right] \times 100$$

where I_{1450} and I_{674} are related to the intensity of internal reference and C–Cl groups, respectively. The substitution degree of 84.2% was calculated.

In addition, the thermal stability of poly(St-VBC), poly(St-VBC)-NH₂, and poly(St-VBC)-NH₂-SO₃H was evaluated by TGA (Figure 5). The TGA/DTG thermograms of poly(St-VBC) showed a significant weight loss in the temperature range of 300–430 °C, which resulted from the overlapping of chlorine removal (as HCl and/or Cl₂) with T_{max} of around 340 °C and decomposition of the main skeleton of the poly(St-VBC) structure with a T_{max} of about 380 °C (Figure 4). For the poly(St-VBC)-NH₂, three weight losses were observed at <170, 190–270, and 340–450 °C (Figure 4). The first one can be related to removing physically adsorbed water/solvents, the second one with T_{max} around 230 °C relates to removing amine groups, and the third one with T_{max} around 410 °C attributes to the decomposition of the main skeleton of the structure, which shifted from 380 to 410 in the absence of chloride function (Figure 5). In the thermogram of poly(St-VBC)-NH₂, the peak related to the chlorine removal was disappeared entirely, and the peak associated with the decomposition of the main skeleton shifted to the higher temperatures, consider shifting of T_{max} from 380 °C for poly(St-VBC) to 410 °C for poly(St-VBC)-NH₂ (Figure 5B). These observations indicate that the chlorine groups were completely replaced with ethylenediamines. Finally, the thermogram of poly(St-VBC)-NH₂-SO₃H showed two main weight losses in the range of 280–350 and 350–455 °C (Figure 5). The first one with T_{max} around 327 °C can be related to removing alkyl sulfonic acid, and the second one with T_{max} around 410 °C relates to the decomposition of the main skeleton of the structure. The disappearance of peaks related to the alkyl amine groups can be a sign of complete

reaction of amine groups of structures with a 1,3-propane sultone (Figure 5B). The thermogravimetric analysis was also conducted for all of the poly(St-VBC)-NH₂-SO₃H(X) samples with different acid content. Based on the results, as the acid content ($X = 100, 200, \text{ and } 500$) increases, the T_{max} of samples decreases from 441 to 431 and 410 °C for $X = 100, 200, 500$, respectively (Figure 5D). Or in other words, the thermal stability of samples decreases with the increase of acid content. Therefore, one can conclude that the –SO₃H groups can catalyze the decomposition of the polymeric matrix of samples during the analysis conditions. These observations indicate that acid fixation with different content on the amine group has been efficiently accomplished. Consequently, the prepared acid–base dual-functional macroporous catalysis exhibited excellent thermal stability up to around 340 °C, indicating that the pores desired for mass transfer in organic catalysis retain their identity and are not collapsed even at high temperature.

Energy-dispersive X-ray (EDX) confirmed the presence of chlorine, amine, and acid functional groups on the prepared macroporous samples (Figure S3). Elemental mapping was also performed to investigate further the elemental composition of the prepared poly(St-VBC)-NH₂-SO₃H. The mapping images showed the presence of carbon, nitrogen, and sulfur and their homogeneous distribution throughout the polymer matrix in the final dual-functional acid–base catalyst (Figure S4).

To confirm further and quantify functional groups (–NH₂ and SO₃H groups) immobilized into/onto the poly(St-VBC) supports, CHNS elemental analysis was conducted. As shown in Table 2, all samples have significant amounts of nitrogen

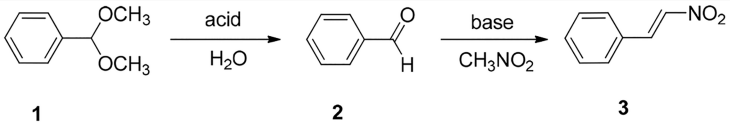
Table 2. CHNS Elemental Analysis of the Prepared Materials

Samples	N (mmol/gr)	S (mmol/gr)	S/N
Poly(St-VBC)-NH ₂	1.47		
Poly(St-VBC)-NH ₂ -SO ₃ H(20)	1.82	1.16	0.68
Poly(St-VBC)-NH ₂ -SO ₃ H(100)	0.83	1.85	2.23
Poly(St-VBC)-NH ₂ -SO ₃ H(200)	0.74	2.24	3.03
Poly(St-VBC)-NH ₂ -SO ₃ H(500)	0.56	2.07	3.69

and sulfur (except for the poly(St-VBC)-NH₂), confirming the successful accomplishment of the functionalization process. The results indicated that the S/N content ratio (which might be attributed to the molar ratio of acid to base) of modified poly(St-VBC)-NH₂-SO₃H(X) samples increases when the added amount of 1,3-propane sultone to the formulation increases. These findings suggest the successful step-by-step functionalization of amine groups in the poly(St-VBC)-NH₂ with propane sultone.

3.4. Catalytic Efficacy of Poly(St-VBC)-NH₂-SO₃H(X) Samples. To investigate how the intrinsic functionalities of an acid/base antagonistic catalyst work cooperatively, two different sets of reactions have been typically evaluated: a nitroaldol reaction and a one-pot deacetalization–nitroaldol reaction. The condensation of nitroalkanes with carbonyl compounds, the so-called Henry reaction, is a well-established and thoroughly verified chemical procedure to generate nitroalkenes, which are essential for the synthesis of pharmaceutical (such as antibacterial, rodent-repelling, and antitumor activities) products. However, selective formation of a nitroalkene using conventional strong bases is difficult since

Table 3. One-Pot Deacetalization–Henry Reaction Using the Prepared Catalysts



Entry	Catalyst	Conversion* of 1 (%)	Yield* of 2 (%)	Yield* of 3 (%)
1	Poly(St-VBC)-NH ₂ -SO ₃ H(20) ^a	100	0	100
2	Poly(St-VBC)-NH ₂ -SO ₃ H(100)	100	58	42
3	Poly(St-VBC)-NH ₂ -SO ₃ H(200)	100	79	21
4	Poly(St-VBC)-NH ₂ -SO ₃ H(500)	100	87	13
5	Poly(St-VBC)-NH ₂ -SO ₃ H(20) ^b	85	5	80
6	Poly(St-VBC)-NH ₂ -SO ₃ H(20) ^c	60	4	56
7	Poly(St-VBC)-NH ₂ -SO ₃ H(20) ^d	10	3	7
8	Poly(St-DVB)-SO ₃ H	100	100	Trace
9	Poly(St-VBC)-NH ₂	6	1	5
10	EDA + Cl-SO ₃ H ^e	Trace	Trace	Trace
11	Poly(St-DVB)-SO ₃ H + EDA ^f	2	2	0
12	Poly(St-VBC)-NH ₂ + Cl-SO ₃ H ^f	100	89	11
13	Poly(St-VBC)-NH ₂ -SO ₃ H(20) + Cl-SO ₃ H ^f	100	100	Trace
14	Poly(St-VBC)-NH ₂ -SO ₃ H(20) + EDA ^f	4	3	1
15	Poly(St-DVB)-SO ₃ H + Poly(St-VBC)-NH ₂	100	2	98
16	Poly(St-DVB)-SO ₃ H + Poly(St-VBC)-NH ₂ ^e	56	11	45
17	Poly(St-VBC)-T(0)-NH ₂ -SO ₃ H (20)	100	57	43
18	Poly(St-VBC)-T(50)-NH ₂ -SO ₃ H (20)	100	43	57
19	Poly(St-VBC)-T(150)-NH ₂ -SO ₃ H (20)	100	27	73

^aBased on GC analysis. Reaction condition: benzaldehyde dimethyl acetal (1 mmol), CH₃NO₂ (5 mL), deionized water (20 μL), catalyst (20 mg), temperature (90 °C), time (24 h); ^aThe initial poly(St-VBC) support is poly(St-VBC)-T=100 in which 100 μL of toluene has been used as the porogenic solvent during the synthesis; ^bReaction time: 18 h. ^cReaction time:14 h. ^dReaction time:6 h. ^e20 mg of each was used as catalyst. ^fTotal catalyst amount; 30 mg = 20 mg solid part + 10 mg homogeneous part.

the conjugate addition of the nitroalkane to the C–C double bond of the nitroalkene gives bis-nitro compounds (nitroalkanes, hydroxylamines, amines, ketones, oximes) in a side reaction. They also react with a variety of nucleophiles and constitute powerful dienophiles for Diels–Alder reactions. It is well-established that solid catalysts with compartmentalized functionalities have the potential to perform notably different reactions in a single pot. To study this concept, we used our prepared poly(St-VBC)-NH₂-SO₃H materials with well-defined porosity and dual functionality in a model cascade reaction of acid-catalyzed hydrolysis of benzaldehyde dimethyl acetal (1) and base-catalyzed Henry reaction between benzaldehyde (2) in the presence of nitromethane to form β-nitrostyrene (3). Considering the suitable porosity, organic nature, which can facilitate the substrate penetration, and high density of strong basic and acidic sites, we hypothesized that the performance of poly(St-VBC)-NH₂-SO₃H as a bifunctional solid catalyst in the case of acid–base-catalyzed tandem reactions involving the deacetalization and subsequent Henry reaction (Table 3) might be promising. To check our hypothesis, we performed multiple control experiments to evaluate the structure–reactivity relationship in the case of our prepared catalysts. For example, we have investigated the influence of type (the first, second, and third type) and concentration of amines and the concentration of acidic sites immobilized in a single heterogeneous catalyst on the deacetylation–Henry cascade reaction. Also, we examined the impact of the presence and absence of porogenic solvent

during the synthesis of the materials on the final catalyst activity in the tandem deacetylation–Henry reaction.

Our investigations revealed that poly(St-VBC)-NH₂-SO₃H-(20) could effectively catalyze the transformation of benzaldehyde dimethyl acetal (1) into 2-nitrovinylbenzene (3) in almost quantitative yield and 100% conversion of 1 within 24 h (Table 3, entry 1). Interestingly, when using poly(St-VBC)-NH₂-SO₃H(100), poly(St-VBC)-NH₂-SO₃H-(200), and poly(St-VBC)-NH₂-SO₃H(500) in the same reaction conditions, although the quantitative conversion of 1 was observed in all cases, the yield of benzaldehyde was gradually increased to 58, 79 and 87%, respectively, and at the same time, the yield of 3 was decreased to 42, 21 and 13%, respectively (Table 3, entries 2–4). These observations are entirely in agreement with the simultaneous enhancement of acid density and decreasing the availability of basic sites in the structure of the catalyst. Based on our results, it seems that the most favorable tuning of acid–base functionality has been achieved in the case of poly(St-VBC)-NH₂-SO₃H(20), which demonstrated the best product yield for β-nitrostyrene in comparison with the other catalysts. Therefore, the subsequent experiments were accomplished using this system. Decreasing the reaction times to 18, 14, and 6 h in the presence of poly(St-VBC)-NH₂-SO₃H(20), under other same reaction conditions, resulted in a gradual drop in both conversion of 1 and yield of 3; while, the selectivity of 3 is still satisfactory even at lower conversions (Table 3, entries 5–7). Comparatively, the employment of the monofunctional poly(St-DVB)-SO₃H (for the synthesis process, please see the Supporting Information)

with strong acidity as a catalyst afforded only the benzaldehyde product (**2**) (Table 3, entry 8), while a negligible amount of **3** was obtained when the reaction was catalyzed by the monofunctional poly(St-VBC)-NH₂ which has only base functionality (Table 3, entry 9). These results, evidently suggested the requirement of coexistence of both strong basic site and active amine functionality in our bifunctional poly(St-VBC)-NH₂-SO₃H catalyst to catalyze the one-pot deacetalization–Henry reaction effectively.

To evaluate the effectiveness of our strategy to prepare the stable supported dual-functional acid–base catalyst, we performed a series of experiments to check the reaction in the presence of homogeneous as well as the mixture of homogeneous and heterogeneous acid and base catalysts. Equal amounts of free chlorosulfonic acid and ethylenediamine as a catalyst system, could not drive the deacetalization–Henry reaction due to the rapid neutralization of catalyst components in the reaction system (Table 3, entry 10). Moreover, a very low conversion of **1** and yield of **3** could be detected when a stoichiometric amount of ethylenediamine was added to Poly(St-DVB)-SO₃H due to the formation of ion pairs, thereby quenching the active acidic sites (Table 3, entry 11). On the other hand, when a mixture of Poly(St-VBC)NH₂ and a stoichiometric amount of Cl-SO₃H was used as the catalyst system, 89% of **2** was produced while the amount of **3** was low (Table 3, entry 12). This could be again attributed to the deactivation of basic sites through the ion-pair formation of functional groups. Interestingly, the same trends were observed when the reaction was accomplished in the presence of Poly(St-VBC)-NH₂-SO₃H(20) and stoichiometric amounts of chlorosulfonic acid or ethylenediamine as catalyst systems (Table 3, entries 13 and 14). All of these results highlight the notion that our developed poly(St-VBC) is excellent solid support with the capability to isolate and stabilize the two antagonistic strong acid and base sites with an elegant nanoengineered site-isolation mechanism and prevent their neutralization during the reaction.

After confirming the stability of both acid and base functional groups in the prepared catalyst system, we then evaluated the possible synergy originating from the coexistence of functional groups in the single support in the one-pot deacetalization–Henry reaction. Our experiments revealed that the physical combination of poly(St-DVB)-SO₃H and poly(St-VBC)-NH₂ catalysts in the one-pot cascade reaction gives the product yield (**3**) of 98% after 24 h reaction at 90 °C (Table 3, entry 15). For a more exact comparison with the reactivity of Poly(St-VBC)-NH₂-SO₃H(20), the same reaction was carried out in a shorter reaction time. The results indicated that the reaction proceeded with 56% conversion, while 45% of **3** was produced in the presence of Poly(St-DVB)-SO₃H + Poly(St-VBC)-NH₂ within 14 h, which is slightly lower than that of Poly(St-VBC)-NH₂-SO₃H(20) (compare entries 6 and 16 in Table 3). This observation confirms the fact that our developed polymeric catalyst support not only stabilizes the two antagonistic acid and base functional groups from chemical neutralization but also can provide a catalytic synergism between these two function groups, thus enhancing the catalytic efficiency in the model one-pot acid/base-catalyzed cascade reactions by decreasing the mass-transfer problems.

In the next part, to examine the role of porogenic solvent employed during the preparation of poly(St-VBC) support and its effect on the physicochemical properties of the synthesized

poly(St-VBC)-NH₂-SO₃H dual functionalized catalysts, the prepared catalysts with different amounts of porogenic solvent (toluene) were assessed in the context of catalyzing the deacetalization–Henry reaction. When the reaction was carried out in the presence of poly(St-VBC)-T(0, 50, 100, 150)-NH₂-SO₃H (with the amount of toluene = 0, 50, 100, and 150 μL, respectively), the complete conversion of **1** was observed in all reactions but 43, 57, 100 and 73%, respectively, of the 2-nitrovinylbenzene product were achieved after 24 h at 90 °C (Table 3, entries 1, 17, and 18). These results well-documented the influence of porogenic solvent on the catalytic activity of the polymer substrate. It seems that by increasing the porogenic solvent content due to the increase in the porosity, roughness, and pore and void size, the product yield enhanced significantly. In contrast, at higher volumes of porogenic solvent (toluene = 150 μL), the substrate's integrity and thermal stability decrease, and this issue might be resulting in the collapse of prepared catalysts and is responsible for a decrease in the final yield of β-nitrostyrene.

To prove that the catalytic activity is originated from covalently bonded base and acid groups rather than the free base and acids leached out, we performed the Sheldon filtration test.³⁵ The studied cascade reactions were performed for 10 h achieving 49% product (**3**) yield. After hot filtration of catalyst from the reaction at this point, the reaction mixture was allowed to stir for another 24 h, but the yield did not increase further. This observation indicated that the prepared poly(St-VBC)-NH₂-SO₃H catalyst is a truly heterogeneous catalyst operating via surface-bond functional groups. Moreover, it can be concluded that both the acidic and basic functional groups are highly stable on the support material and undergo negligible leaching from the support even at 90 °C within 24 h.⁸³

Finally, we checked the recoverability of our developed catalyst in the model reaction under the optimized reaction conditions. Poly(St-VBC)-NH₂-SO₃H can be readily recycled by filtration and reused at least four times without considerable loss of its catalytic activity (Figure 6). A slight decreasing in the catalytic activity is likely due to small losing the mass of catalyst during its repeated filtration and transferring to the reaction pot for the next runs. The high recoverability of the catalyst could be attributed to the tightly covalent anchoring of catalytically active sites and robust framework of the support.

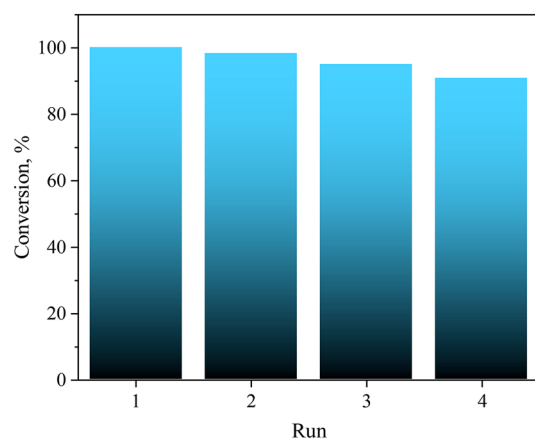


Figure 6. Recycling of poly(St-VBC)-NH₂-SO₃H(20) catalyst in the one-pot cascade reaction.

4. CONCLUSION

In summary, we developed an efficient and simple high internal phase emulsions polymerization method for the synthesis of a series of macroporous polymers using vinylbenzyl chloride (VBC) and styrene (St) as monomers, divinylbenzene (DVB) as a cross-linking agent, and toluene as the porogenic solvent. We studied the effect of various amounts of porogenic solvent on the structural properties of the prepared polymer. The results indicated that the increase in toluene amount (as the porogenic solvent) in the formulation increased the surface area, pore, and void sizes. In the next part, the prepared macroporous polymers were modified with ethylenediamine and subsequently with 1,3-propane sultone to give a dual-functionalized acid–base heterogeneous catalyst. The prepared catalyst demonstrated outstanding activity in the one-pot production of β -nitrostyrene from benzaldehyde dimethyl acetal under cascade reactions comprising acid-catalyzed deacetalization and base-catalyzed Henry reactions. The catalyst showed excellent catalytic performance with 100% substrate conversion and 100% yield of the final product in the mentioned transformation. Interestingly, it was found that when the same reaction was accomplished using both/either homogeneous acid and/or base catalysts, the reaction was not proceeded efficiently, confirming the fact that our support provides a suitable platform for single-site isolation and stabilization of both active acidic and basic functional groups in the channels and prevent them from deactivation through the chemical neutralization. In addition, our experiments confirmed that the concomitant immobilization of two acid and base catalysts on a single polymeric support could provide a catalytic synergism between these antagonistic sites in the model cascade deacetalization–Henry reaction, besides their stabilization against the chemical neutralization. The catalyst could be recovered easily by simple filtration and was reusable for at least four sequential runs without significant losing activity. All in all, the high catalytic activity, recoverability, stability, and durability of the catalyst during the long reaction period might be attributed to the developed support's excellent chemical and physical properties. For example, its highly stable nature prevents the catalyst against decomposition. Its suitable structural features such as the interconnected microchannels and organic nature facilitate the penetration of all substrates to the proximity of active sites without any considerable diffusion problems. On the other hand, the covalently bounded active sites on the support is another crucial point in providing the observed catalyst's stability. We think that the developed material in this study might attract attention in the future among the material and catalyst designers since it provides a new route for developing site-isolated acid–base dual-functionalized heterogeneous catalysts.

■ ASSOCIATED CONTENT

SI Supporting Information

The Supporting Information is available free of charge at <https://pubs.acs.org/doi/10.1021/acsomega.2c02973>.

Synthesis of poly(St-VBC)-SO₃H through HIPE templating, histograms of pore and void distributions fitted by Gaussian equation for sample with different porogen content [poly(St-VBC)-T=0, poly(St-VBC)-T=50, poly(St-VBC)-T=100, poly(St-VBC)-T=150]; energy-dispersive X-ray (EDX) spectra of poly(St-VBC), poly(St-VBC)-NH₂, and poly(St-VBC)-NH₂-SO₃H(20); ele-

mental mapping images of poly(St-VBC)-NH₂-SO₃H(20) (PDF)

■ AUTHOR INFORMATION

Corresponding Author

Nasser Nikfarjam – Department of Chemistry, Institute for Advanced Studies in Basic Sciences (IASBS), Zanjan 45137-66731, Iran; Present Address: Department of Chemical Engineering, College of Engineering and Computing, University of South Carolina, Columbia SC 29208; orcid.org/0000-0002-5995-7734; Phone: +98 24 33153132; Email: nikfarjam@iasbs.ac.ir; Fax: +98 24 33253232

Authors

Saeed Ghanooni – Department of Chemistry, Institute for Advanced Studies in Basic Sciences (IASBS), Zanjan 45137-66731, Iran

Babak Karimi – Department of Chemistry, Institute for Advanced Studies in Basic Sciences (IASBS), Zanjan 45137-66731, Iran; Research Center for Basic Sciences & Modern Technologies (RBST), Institute for Advanced Studies in Basic Sciences (IASBS), Zanjan 45137-66731, Iran

Complete contact information is available at: <https://pubs.acs.org/10.1021/acsomega.2c02973>

Notes

The authors declare no competing financial interest.

■ ACKNOWLEDGMENTS

The authors are grateful to the Institute for Advanced Studies in Basic Sciences (IASBS) for financial support of this work.

■ REFERENCES

- (1) Wu, D.; Xu, F.; Sun, B.; Fu, R.; He, H.; Matyjaszewski, K. Design and Preparation of Porous Polymers. *Chemical reviews*. **2012**, *112* (7), 3959–4015.
- (2) Karimi, B.; Artelli, Z.; Mohammadi, F.; Mansouri, F. An Amphiphilic Mesoporous Polymer Comprising a “Built-in” Imidazolium Ionic Liquid via Nanocasting Method as a Novel Catalyst Support with Combined Prospects. *Chemistry Select*. **2019**, *4* (1), 347–356.
- (3) Karimi, B.; Marefat, R.; Hasannia, M.; Akhavan, F. Imidazolyl-Functionalized Ordered Mesoporous Polymer from Nanocasting as an Effective Support for Highly Dispersed Palladium Nanoparticles in the Heck Reaction. *ChemCatChem*. **2016**, *8* (15), 1–9.
- (4) de Jong, J.; Ankone, B.; Lammertink, R. G. H.; Wessling, M. New Replication Technique for the Fabrication of Thin Polymeric Microfluidic Devices with Tunable Porosity. *Lab on a Chip*. **2005**, *5* (11), 1240–1247.
- (5) Yao, C.; Qi, L.; Jia, H.; Xin, P.; Yang, G.; Chen, Y. A Novel Glycidyl Methacrylate-Based Monolith with Sub-micron Skeletons and Well-Defined Macropores. *Journal of Materials Chemistry*. **2009**, *19* (6), 767–772.
- (6) Lovelady, E.; Kimmins, S. D.; Wu, J.; Cameron, N. R. Preparation of Emulsion-Templated Porous Polymers Using Thiol–ene and Thiol–yne Chemistry. *Polymer Chemistry*. **2011**, *2* (3), 559–562.
- (7) Lazzari, M.; López-Quintela, M. A. Block Copolymers as a Tool for Nanomaterial Fabrication. *Adv. Mater.* **2003**, *15* (19), 1583–1594.
- (8) Hong, K. H.; Oh, K. W.; Kang, T. J. Preparation of Conducting Nylon-6 Electrospun Fiber Webs by the in Situ Polymerization of Polyaniline. *J. Appl. Polym. Sci.* **2005**, *96* (4), 983–991.
- (9) Lau, T. H.; Wong, L. L.; Lee, K. Y.; Bismarck, A. Tailored for Simplicity: Creating High Porosity, High Performance Bio-Based

- Macroporous Polymers from Foam Templates. *Green Chemistry*. **2014**, *16* (4), 1931–1940.
- (10) Barbetta, A.; Dentini, M.; Leandri, L.; Ferraris, G.; Coletta, A. Reactive & Functional Polymers Synthesis and Characterization of Porous Glycidylmethacrylate – Divinylbenzene Monoliths Using the High Internal Phase Emulsion Approach. *React. Funct. Polym.* **2009**, *69* (9), 724–736.
- (11) Zou, S.; Yang, Y.; Liu, H.; Wang, C. Colloids and Surfaces A: Physicochemical and Engineering Aspects Synergistic Stabilization and Tunable Structures of Pickering High Internal Phase Emulsions by Nanoparticles and Surfactants. *Colloids Surfaces A Physicochem. Eng. Asp.* **2013**, *436*, 1–9.
- (12) Lissant, K. J. The Geometry of High-Internal-Phase-Ratio Emulsions. *Journal of colloid and interface science*. **1966**, *22* (5), 462–468.
- (13) Princen, H. M. Highly Concentrated Emulsions. I. Cylindrical Systems. *J. Colloid Interface Sci.* **1979**, *71* (1), 55–66.
- (14) Silverstein, M. S. (2014). PolyHIPEs: Recent Advances in Emulsion-Templated Porous Polymers. *Prog. Polym. Sci.* **2014**, *39* (1), 199–234.
- (15) Manley, S. S.; Graeber, N.; Grof, Z.; Menner, A.; Hewitt, G. F. New Insights into the Relationship between Internal Phase Level of Emulsion Templates and Gas – Liquid Permeability of Interconnected Macroporous Polymers. *Soft Matter*. **2009**, *5* (23), 4780–4787.
- (16) Barbetta, A.; Cameron, N. R. Morphology and Surface Area of Emulsion-Derived (PolyHIPE) Solid Foams Prepared with Oil-Phase Soluble Porogenic Solvents: Span 80 as Surfactant. *Macromolecules*. **2004**, *37* (9), 3188–3201.
- (17) Barbetta, A.; Cameron, N. R. Morphology and Surface Area of Emulsion-Derived (PolyHIPE) Solid Foams Prepared with Oil-Phase Soluble Porogenic Solvents: Three-Component Surfactant System. *Macromolecules*. **2004**, *37* (9), 3202–3213.
- (18) Barbetta, A.; Cameron, N. R.; Cooper, S. J. High Internal Phase Emulsions (HIPEs) Containing Divinylbenzene and 4-Vinylbenzyl Chloride and the Morphology of the Resulting PolyHIPE Materials. *Chemical Communications*. **2000**, *3*, 221–222.
- (19) Williams, J. M. (1991). High Internal Phase Water-in-Oil Emulsions: Influence of Surfactants and Cosurfactants on Emulsion Stability and Foam Quality. *Langmuir*. **1991**, *7* (7), 1370–1377.
- (20) Williams, J. M.; Gray, A. J.; Wilkerson, M. H. Emulsion Stability and Rigid Foams from Styrene or Divinylbenzene Water-in-Oil Emulsions. *Langmuir*. **1990**, *6* (2), 437–444.
- (21) Williams, J. M.; Wroblewski, D. A. Spatial Distribution of the Phases in Water-in-Oil Emulsions. Open and Closed Microcellular Foams from Cross-Linked Polystyrene. *Langmuir*. **1988**, *4* (3), 656–662.
- (22) Menner, A.; Bismarck, A. New Evidence for the Mechanism of the Pore Formation in Polymerising High Internal Phase Emulsions or Why PolyHIPEs Have an Interconnected Pore Network Structure. *Macromolecular symposia*. **2006**, *242* (1), 19–24.
- (23) Cameron, N. R. High Internal Phase Emulsion Templating as a Route to Well-Defined Porous Polymers. *Polymer*. **2005**, *46* (5), 1439–1449.
- (24) Ma, L.; Luo, X.; Cai, N.; Xue, Y.; Zhu, S.; Fu, Z.; Yu, F. Applied Surface Science Facile Fabrication of Hierarchical Porous Resins via High Internal Phase Emulsion and Polymeric Porogen. *Appl. Surf. Sci.* **2014**, *305*, 186–193.
- (25) Cameron, N. R.; Barbetta, A. The Influence of Porogen Type on the Porosity, Surface Area and Morphology of Poly(Divinylbenzene) PolyHIPE Foams. *Journal of Materials Chemistry*. **2000**, *10* (11), 2466–2471.
- (26) Koroleva, M. Y.; Shirokikh, S. A.; Zagoskin, P. S.; Yurtov, E. V.; Malgras, V.; Tang, J.; Wang, J.; Kim, J.; Torad, N. L.; Dutta, S.; et al. Poly (HIPE) Morphology, Crosslink Density, and Mechanical Properties Influenced by Surfactant Concentration and Composition. *Colloids Surfaces A* **2019**, *77* (S88), 123913.
- (27) Bhum, Z. Polyhipe Foam Materials as Filtration Media. *Filtration & separation*. **1995**, *32* (3), 245–251.
- (28) Foudazi, R. HIPEs to PolyHIPEs. *React. Funct. Polym.* **2021**, *164*, 104917.
- (29) Rohm, K.; Manas-zloczower, I.; Feke, D.; Koroleva, M. Y.; Shirokikh, S. A.; Zagoskin, P. S.; Yurtov, E. V.; Malgras, V.; Tang, J.; Wang, J.; et al. Poly (HIPE) Morphology, Crosslink Density, and Mechanical Properties Influenced by Surfactant Concentration and Composition. *Colloids Surfaces A* **2019**, *583*, 123913.
- (30) Grondal, C.; Jeanty, M. Organocatalytic Cascade Reactions as a New Tool in Total Synthesis. *Nat. Chem.* **2010**, *2* (3), 167–178.
- (31) Lohr, T. L.; Marks, T. J. Orthogonal Tandem Catalysis. *Nat. Publ. Gr.* **2015**, *7* (6), 477–482.
- (32) Xu, H.; Zheng, X.; Huang, Y.; Wang, H.; Du, Q. Interconnected Porous Polymers with Tunable Pore Throat Size Prepared via Pickering High Internal Phase Emulsions. *Langmuir*. **2016**, *32* (1), 38–45.
- (33) Womble, C. T.; Kuepfert, M.; Cohen, A. E.; Weck, M. Multicompartment Polymeric Nanoreactors for Non-Orthogonal Cascade Catalysis. *Macromol. Rapid Commun.* **2019**, *40* (1), 1800580.
- (34) Wilson, Y. M.; Du, M.; Ghislieri, D.; Churakova, E.; Quinto, T.; Kno, L.; Hollmann, F.; Turner, N. J.; Ward, T. R. Synthetic Cascades Are Enabled by Combining Biocatalysts with Artificial Metalloenzymes. *Nature Chemistry*. **2012**, *5* (2), 93–99.
- (35) Zhao, T.; Yao, Y.; Wang, M.; Chen, R.; Yu, Y.; Wu, F.; Zhang, C. Preparation of MnO₂-Modified Graphite Sorbents from Spent Li-Ion Batteries for Lead, Cadmium and Silver Contaminated Water Treatment. *ACS applied materials & interfaces*. **2017**, *9* (30), 25369–25376.
- (36) Wei, W.; Li, A.; Pi, S.; Wang, Q.; Zhou, L.; Yang, J.; Ma, F.; Ni, B. Synthesis of Core-Shell Magnetic Nano-Composite Fe₃O₄ @ Microbial Extracellular Polymeric Substances for Simultaneous Redox Sorption and Recovery of Silver Ions as Silver Nanoparticles. *ACS Sustainable Chemistry & Engineering*. **2017**, *6* (1), 1–28.
- (37) Zhu, Y.; Zheng, Y.; Wang, F.; Wang, A. Monolithic Supramacroporous Hydrogel Prepared from High Internal Phase Emulsions (HIPEs) for Fast Removal of Cu²⁺ and Pb²⁺. *Chem. Eng. J.* **2016**, *284*, 422–430.
- (38) Dinker, M. K.; Ajithkumar, T. G.; Kulkarni, P. S. - Proline Functionalized Dicationic Framework of Bifunctional Mesoporous Organosilica for the Simultaneous Removal of Lead and Nitrate Ions. *ACS Sustainable Chemistry & Engineering*. **2017**, *5* (5), 4188–4196.
- (39) Zhu, H.; Tan, X.; Tan, L.; Zhang, H.; Liu, H.; Fang, M.; Hayat, T.; Wang, X. Magnetic Porous Polymers Prepared Via High Internal Phase Emulsions for Efficient Removal of Pb²⁺ and Cd²⁺ Magnetic Porous Polymers Prepared Via High Internal Phase. *ACS Sustainable Chemistry & Engineering*. **2018**, *6* (4), 5206–5213.
- (40) Ko, Y. G.; Lee, H. J.; Kim, J. Y.; Choi, U. S. Hierarchically Porous Aminosilica Monolith as a CO₂ Adsorbent. *ACS Applied Materials & Interfaces*. **2014**, *6* (15), 12988–12996.
- (41) Wang, Q.; Liu, Y.; Chen, J.; Du, Z.; Mi, J. Control of Uniform and Interconnected Macroporous Structure in PolyHIPE for Enhanced CO₂ Adsorption/Desorption Kinetics Control of Uniform and Interconnected Macroporous Structure in PolyHIPE for Enhanced CO₂ Adsorption/Desorption Kinetics. *Environmental Science & Technology*. **2016**, *50* (14), 7879–7888.
- (42) Zhang, N.; Zhong, S.; Zhou, X.; Jiang, W.; Wang, T.; Fu, J. Superhydrophobic P (St-DVB) Foam Prepared by the High Internal Phase Emulsion Technique for Oil Spill Recovery. *Chem. Eng. J.* **2016**, *298*, 117–124.
- (43) Tunc, Y.; Hasirci, N.; Ulubayram, K. Synthesis of Emulsion-Templated Acrylic-Based Porous Polymers: from Brittle to Elastomeric. *Soft Materials*. **2012**, *10* (4), 449–461.
- (44) Fujisawa, K.; Humbert-droz, M.; Letrune, R.; Vauthey, E.; Wesolowski, T. A.; Sakai, N.; Matile, S. Ion Pair – π Interactions. *J. Am. Chem. Soc.* **2015**, *137* (34), 11047–11056.
- (45) Shi, G.; Liu, J.; Wang, C.; Song, B.; Tu, Y.; Hu, J.; Fang, H. Ion Enrichment on the Hydrophobic Carbon-Based Surface in Aqueous Salt Solutions Due to Cation- π Interactions. *Scientific reports*. **2013**, *3* (1), 1–5.

- (46) Shylesh, S.; Wagener, A.; Seifert, A.; Ernst, S.; Thiel, W. R. Mesoporous Organosilicas with Acidic Frameworks and Basic Sites in the Pores: An Approach to Cooperative Catalytic Reactions. *Angewandte Chemie International Edition*. **2010**, *49* (1), 184–187.
- (47) Jun, S. W.; Shokouhimehr, M.; Jun, D.; Jang, Y.; Hyeon, T. Mesoporous Silica Supported Acid – Base Catalysts for Tandem Reactions †. *Chemical Communications*. **2013**, *49* (71), 7821–7823.
- (48) Puthiaraj, P.; Chung, Y.; Ahn, W. Dual-Functionalized Porous Organic Polymer as Reusable Catalyst for One-Pot Cascade C C Bond-Forming Reactions. *Mol. Catal*. **2017**, *441*, 1–9.
- (49) Yang, Y.; Liu, X.; Li, X.; Zhao, J.; Bai, S.; Liu, J.; Yang, Q. A Yolk – Shell Nanoreactor with a Basic Core and an Acidic Shell for Cascade Reactions. *Angew. Chem., Int. Ed.* **2012**, *51* (36), 9164–9168.
- (50) Pillai, K. V.; Renneckar, S. Cation - π Interactions as a Mechanism in Technical Lignin Adsorption to Cationic Surfaces. *Biomacromolecules*. **2009**, *10* (4), 798–804.
- (51) Awual, R.; Miyazaki, Y.; Taguchi, T.; Shiwaku, H.; Yaita, T. Encapsulation of Cesium from Contaminated Water with Highly Selective Facial Organic-Inorganic Mesoporous Hybrid Adsorbent. *Chem. Eng. J.* **2016**, *291*, 128–137.
- (52) Rao, J. S.; Zipse, H.; Sastry, G. N. Explicit Solvent Effect on Cation - π Interactions: A First Principle Investigation. *J. Phys. Chem. B* **2009**, *113* (20), 7225–7236.
- (53) Liu, J.; Li, J.; Yang, X.; Song, Q.; Bai, C.; Shi, Y.; Zhang, L.; Liu, C.; Li, S.; Ma, L. Facile Preparation of Polyphenolic Hydroxyl Functionalized Uranium-Selective Chelating Sorbent: Simple Oxidation of Styrene – Divinylbenzene Copolymer Microparticles by Hummers Method. *Mater. Lett.* **2013**, *97*, 177–180.
- (54) Online, V. A.; Zhang, Y. Dual Functionalization of Porous Aromatic Heterogeneous Cascade Catalysis †. *Chemical Communications*. **2014**, *50* (62), 8507–8510.
- (55) Gebbie, M. A.; Wei, W.; Schrader, A. M.; Cristiani, T. R.; Dobbs, H. A.; Idso, M.; Chmelka, B. F.; Waite, J. H.; Israelachvili, J. N. Cation – π Interactions. *Nat. Chem.* **2017**, *9* (5), 473–479.
- (56) Tan, H.; Wei, J.; Sun, G.; Mu, C.; Lin, W.; Ngai, T. Interconnected Macroporous 3D Scaffolds Templated from Gelatin Nanoparticle-Stabilized High Internal Phase Emulsions for Biomedical Applications. *Soft Matter*. **2017**, *13* (21), 3871–3878.
- (57) Vernekar, D.; Jagadeesan, D. (2015). Tunable Acid–Base Bifunctional Catalytic Activity of FeOOH in an Orthogonal Tandem Reaction. *Catalysis Science & Technology*. **2015**, *5* (8), 4029–4038.
- (58) Guo, Y.; Feng, L.; Wang, X.; Zhang, X. Integration of Yolk–Shell Units into a Robust and Highly Reactive Nanoreactor: a Platform for Cascade Reactions. *Chemical Communications*. **2019**, *55* (21), 3093–3096.
- (59) Shang, F.; Sun, J.; Liu, H.; Wang, C.; Guan, J.; Kan, Q. One-Pot Cascade Reactions Catalyzed by Acid – Base Mesoporous MCM-41 Materials. *Mater. Res. Bull.* **2012**, *47* (3), 801–806.
- (60) Shang, F.; Sun, J.; Wu, S.; Liu, H.; Guan, J.; Kan, Q. Journal of Colloid and Interface Science Direct Synthesis of Acid – Base Bifunctionalized Hexagonal Mesoporous Silica and Its Catalytic Activity in Cascade Reactions. *J. Colloid Interface Sci.* **2011**, *355* (1), 190–197.
- (61) Gianotti, E.; Diaz, U.; Veltz, A.; Corma, A. Designing Bifunctional Acid–Base Mesoporous Hybrid Catalysts for Cascade Reactions. *Catalysis Science & Technology*. **2013**, *3* (10), 2677–2688.
- (62) You, C.; Yu, C.; Yang, X.; Li, Y.; Huo, H.; Wang, Z.; Lin, K. Double-Shell Hollow Mesoporous Silica Nanospheres as an Acid–Base Bifunctional Catalyst for Cascade Reactions. *New J. Chem.* **2018**, *42* (6), 4095–4101.
- (63) Javad Kalbasi, R.; Mansouri, S.; Mazaheri, O. Into the Pores of Hierarchical MFI Zeolite as an Acid – Base Bifunctional Catalyst for One Pot C – C Bond Cascade Reactions. *Res. Chem. Intermed.* **2018**, *44* (5), 3279–3291.
- (64) Gao, J.; Zhang, X.; Lu, Y.; Liu, S.; Liu, J. Selective Functionalization of Hollow Nanospheres with Acid and Base Groups for Cascade Reactions. *Chemistry—A European Journal*. **2015**, *21* (20), 1–6.
- (65) Wang, X.; Zhang, L.; Guo, Z.; Shi, Y.; Zhou, Y.; Wang, J. Applied Surface Science Synergistic Catalysis of One-Pot Cascade Reactions by Acidic and Basic Binary Porous Polymers. *Appl. Surf. Sci.* **2019**, *478*, 221–229.
- (66) Wang, K.; Jia, Z.; Yang, X.; Wang, L.; Gu, Y.; Tan, B. Acid and Base Coexisted Heterogeneous Catalysts Supported on Hypercrosslinked Polymers for One-Pot Cascade Reactions. *J. Catal.* **2017**, *348*, 168–176.
- (67) Yang, H.; Fu, L.; Wei, L.; Liang, J.; Binks, B. P. Compartmentalization of Incompatible Reagents Within Pickering Emulsion Droplets for One-Pot Cascade Reactions. *J. Am. Chem. Soc.* **2015**, *137* (3), 1362–1371.
- (68) Chen, C.; Janoszka, N.; Wong, C. K.; Gramse, C.; Weberskirch, R.; Gröschel, A. H. Scalable and Recyclable All-Organic Colloidal Cascade Catalysts. *Angewandte Chemie International Edition*. **2021**, *60* (1), 237–241.
- (69) Ressam, I.; El, A.; Lahcini, M.; Luinstra, G. A.; Perrot, H.; Sel, O. ScienceDirect Enhanced Proton Transport Properties of Nafion via Functionalized Halloysite Nanotubes. *Int. J. Hydrogen Energy*. **2018**, *43* (40), 1–14.
- (70) Haibey, P.; Huxham, I. M.; Rowatt, B.; Sherrington, D. C.; Tetley, L. Synthesis and Ultrastructural Studies of Styrene-Divinylbenzene PolyHIPE polymers. *Macromolecules*. **1991**, *24* (1), 117–121.
- (71) Cameron, N. R.; Barbeta, A. The Influence of Porogen Type on the Porosity, Surface Area and Morphology of Poly (divinylbenzene) PolyHIPE Foams. *Journal of Materials Chemistry*. **2000**, *10* (11), 2466–2471.
- (72) Kavousi, F.; Nikfarjam, N. Highly Interconnected Macroporous Structures Made from Starch Nanoparticle-Stabilized Medium Internal Phase Emulsion Polymerization for Use in Cell Culture. *Polymer (Guildf)*. **2019**, *180*, 121744.
- (73) Sufi-Maragheh, P.; Nikfarjam, N.; Deng, Y.; Taheri-Qazvini, N. Pickering Emulsion Stabilized by Amphiphilic PH-Sensitive Starch Nanoparticles as Therapeutic Containers. *Colloids and Surfaces B: Biointerfaces*. **2019**, *181*, 244–251.
- (74) Bakeshlou, Z.; Nikfarjam, N. Thermoregulating Papers Containing Fabricated Microencapsulated Phase Change Materials through Pickering Emulsion Templating. *Ind. Eng. Chem. Res.* **2020**, *59* (46), 20253–20268.
- (75) Barbeta, A.; Cameron, N. R. Morphology and Surface Area of Emulsion-Derived (PolyHIPE) Solid Foams Prepared with Oil-Phase Soluble Porogenic Solvents: Three-Component Surfactant System. *Macromolecules*. **2004**, *37* (9), 3202–3213.
- (76) Liang, N.; Liu, Y.; Liao, X.; Luo, Z.; Chen, D.; Liu, X.; Zhang, H. Preparation and Characterization of Anion-Exchange Membranes Derived from Poly (Vinylbenzyl Chloride-co-Styrene) and Intercalated Montmorillonite. *Polymers for Advanced Technologies*. **2017**, *28* (6), 728–735.
- (77) Karimi, B.; Khalkhali, M. Silica Functionalized Sulfonic Acid as a Recyclable Interphase Catalyst for Chemoselective Thioacetalization of Carbonyl Compounds in Water. *Journal of Molecular Catalysis A: chemical*. **2007**, *271*, 75–79.
- (78) Zareyee, D.; Karimi, B. A Novel and Highly Efficient Method for the Silylation of Alcohols with Hexamethyldisilazane (HMDS) Catalyzed by Recyclable Sulfonic Acid-Functionalized Ordered Nanoporous Silica. *Tetrahedron Lett.* **2007**, *48* (7), 1277–1280.
- (79) Gill, C. S.; Price, B. A.; Jones, C. W. Sulfonic Acid-Functionalized Silica-Coated Magnetic Nanoparticle Catalysts. *J. Catal.* **2007**, *251* (1), 145–152.
- (80) Manjunathan, P.; Kumar, M.; Churipard, S. R.; Sivasankaran, S.; Shanbhag, G. V.; Maradur, S. P. Catalytic Etherification of Glycerol to Tert-Butyl Glycerol Ethers Using Tert-Butanol Over Sulfonic Acid Functionalized Mesoporous Polymer. *RSC advances*. **2016**, *6* (86), 82654–82660.
- (81) Zhang, Y.; Li, B.; Ma, S. Dual Functionalization of Porous Aromatic Frameworks as a new Platform for Heterogeneous Cascade Catalysis. *Chemical Communications*. **2014**, *50* (62), 8507–8510.

(82) Evecen, M.; Tanak, H. Quantum Chemical Studies on the Molecular Structure, Spectroscopic and Electronic Properties of (6-Methoxy-2-Oxo-2H-Chromen-4-yl)-Methyl Pyrrolidine-1-Carbodithioate. *Materials Science-Poland*. **2016**, *34* (4), 886–904.

(83) Yavuz, E.; Cherkasov, N.; Degirmenci, V. Acid and Base Catalysed Reactions in One Pot with Site-Isolated PolyHIPE Catalysts. *RSC Adv.* **2019**, *9* (15), 8175–8183.